International Congress on Ultrasonics, Universidad de Santiago de Chile, January 2009

Strategies for single particle manipulation using acoustic radiation forces and external tools

Stefano Oberti, Adrian Neild[a], Dirk Möller*, Jurg Dual

Institute of Mechanical Systems – Center of Mechanics, ETH Zurich, Tannenstrasse 3, 8292 Zurich, Switzerland
[a] Dept. of Mechanical and Aerospace Engineering, Monash University, VIC 3800, Australia

Abstract

The use of primary acoustic radiation forces has been shown to be a valid technique for the handling of micron sized suspended particles, such as beads or biological cells. These forces arise as a nonlinear effect when an acoustic wave or vibration, which is set up in the fluid by exciting to resonance the system containing the suspension, interacts with the particles. The typical frequencies (upper kHz - lower MHz range) and the periodicity (in the range of hundreds of micrometers) of the acoustic field make this technique particularly suited for the handling of particles within microfluidic systems.
A variety of devices for separation, fractionation, trapping and positioning of beads or biological cells, working both in batch [1-2] or fluid flow [3-4] mode, have been proposed. With the exception of the ports used to inject or remove the sample or the carrier medium, these systems can be considered as closed systems. Nevertheless, access to the particles with external tools is sometimes needed after acoustic manipulation has been performed. For instance, particles or cells pre-positioned in a sequence along the centerline of a channel using acoustic radiation forces need to be removed from it using a microgripper for further handling. Furthermore, in the field of crystallography research protein crystals have to be placed one by one onto a nylon loop prior to X-ray analysis with synchrotron radiation. This is usually done using the loop to pick up the crystal from the solution where it has been growing with other ones. As this process is sometimes repeated for a large number of crystals there are efforts to automate it. To this purpose it would be advantageous to bring the crystals spatially separated into a known position where they than can be sequentially collected with the loop.
Here strategies for single particle manipulation are presented combining the effects of acoustic fields, fluid flow, surface tension and external tools. They are discussed by means of numerical results from FE-simulations of both two and three dimensional models as well as corresponding experiments.

Keywords: particle manipulation; cell manipulation; crystal manipulation; acoustic manipulation; FE-modeling; Gor'kov

1. Introduction

Due to the long range nature of the acoustic force field, to which all the suspended particles respond, acoustic manipulation is highly suited for the simultaneous handling of large amounts of particles. In contrast, its potential as

---

* Corresponding author. Tel.: +41- 44 - 632 61 06; fax: +41- 44 - 632 11 45.
  E-mail address: dirk.moeller@imes.mavt.ethz.ch.

a manipulation technique for single particles will be demonstrated here, by showing that large particles (diameter above 50 μm) can be positioned in specially designed systems, in such a way that they are individually accessible.

The idea of a combined use of acoustic manipulation and mechanical handling consists in bringing particles in sequence into a known location using acoustic radiation forces and from there remove them one by one using a tool. For this, both the lateral and longitudinal position have to be controlled, whereas vertical control is indirectly guaranteed as the particles can sit on the bottom surface. Moreover, transport of particles to the location where they are picked up with the tool can be achieved using drag forces arising from laminar flow. Such a combination offers the possibility of some degree of automation in the manipulation process of particles, as the tool can be controlled with a robotic system.

Firstly, previous work on the combined use of acoustic pre-positioning and successive manipulation with a capacitively actuated microgripper is reviewed. Then, a novel device conceived for the manipulation of protein crystals before crystallographic analysis is illustrated. The finite element simulations, in two dimensions for the first case and three for the second, gives rise to a discussion of the limits of the first approach and points out the necessity of the second one.

2. Manipulation of previously acoustically aligned particles using a microgripper

2.1. Experimental setup and method

A 5 mm long channel with a 0.2×1 mm rectangular cross section, fabricated by dry etching a 300 μm silicon wafer has been used for this experiment (Fig. 1). Sealing and in turn optical access is provided by a 1 mm thick glass plate, attached using two components epoxy. One end was cut straight, leaving a rectangular water meniscus as boundary, held by surface tension forces. This way, particles close to the interface can be reached by the microgripper inserted through the meniscus. At the other extremity of the channel a circular well, connected with the channel and having the same depth, acts as reservoir for the particle suspension. Excitation to vibration and in turn setting up of an acoustic standing wave field when the resonant condition for the whole system is matched is realized by means of a piezoelectric plate covering the whole width of the device and cut at two locations in correspondence to the channel walls. The aim of such cuts is that of decoupling the vibration of the piezoelectric confined within them and the rest of the plate, to concentrate all the energy in the channel. For this device a strip electrode configuration, as introduced in [1], has been adopted; the harmonic electrical signal has been applied only to a narrow stripe, defined on the lower side of the piezoelectric in the region between the two cuts by removing the conductive electrode layer along the whole length of the plate, using a wafer saw. The other part of the lower electrode and the electrode in contact with the silicon has been grounded. Keeping the active piezoelectric part to a minimum size, together with the low operation frequencies and the fact that the transducer was usually kept active only for short periods, helped to minimize any heat generation. In fact no detrimental effects were observed during the experiments. The resulting actuation is not symmetric with respect to the *y-z* plane, passing through the center of the fluid cavity, leading to various pressure fields. Depending on the frequency anti symmetric pressure fields with an odd number of trapping planes can be set up, i.e with always a trapping plane along the centerline of the channel, as required in order for the microgripper to be able to reach each particle.

The microgripper itself has a capacitively actuated finger which can be activated by applying a DC voltage and has been fabricated according to the procedure described by Beyeler *et al* in [5].

For operation the acoustic device was placed under a microscope (Olympus ZSH), so that observation of the manipulation process and the motion of the microgripper could be followed from above through the glass plate using a CCD camera (Sony CCD-Iris, Model SSC-M370CE) with a frame grabber (Newport, PC-IMAQ 1408) for data acquisition into a PC. In the experiments 74 μm particles (Duke Scientific) were loaded into the channel, by depositing a droplet of suspension in the reservoir and waiting until the channel is filled by capillary forces. Excitation of the piezoelectric transducer mounted on the acoustic device was performed with a Stanford Research DS345 function generator and an amplifier (ENI 2100L). The microgripper was mounted on a *xyz*-stage (Newport MM4006), operated manually with a joystick together with a LabView program to define the speed.
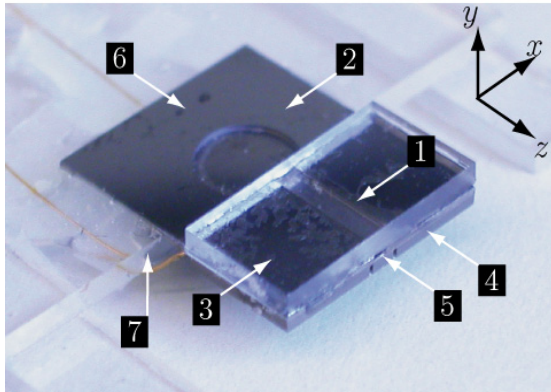
Fig. 1 Acoustic device consisting in a three layer structure: a 1 mm wide, 200 µm deep channel (1) etched into a 300 µm thick silicon layer (2), sealed on the top with a 1 mm thick glass plate (3). On the backside a 500 µm piezoelectric transducer (4) has been attached. One end (5) has been cut straight in order for a microgripper lying in the x-z plane to enter the channel from there along the z-direction and remove the particles collected in the channel. Operation is performed by loading the channel with particle suspension through the reservoir (6), exploiting capillary forces, and excite the system to resonance by applying a harmonic electrical signal to a narrow area of the lower electrode. The device is mounted on a glass frame (7).
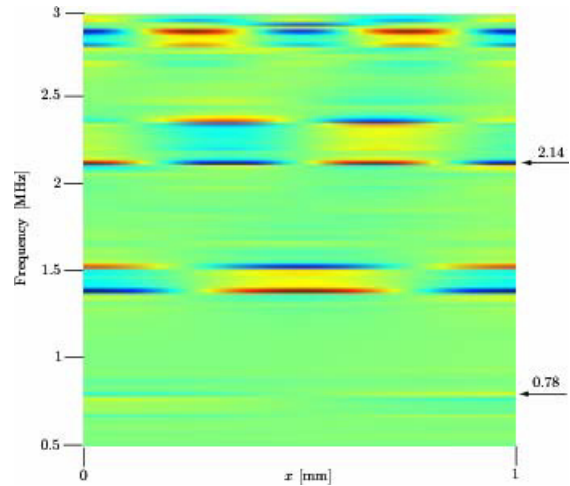
Fig.2 Simulated pressure amplitude along the lower boundary of the channel plotted for a frequency range from 500 to 3000 kHz. As one line of particles along the channel centerline is required for this application, the frequencies of interest are 780 kHz and 2140 kHz, at which one and three lines of particles are formed, respectively. According to the Gor'kov theory [9], in a two dimensional approach, the trapping locations correspond in fact to the pressure nodes.

2.2. FE-Modeling (2D)

The response of the acoustic device to harmonic electrical excitation of the piezoelectric has been modeled in two dimensions (*x-y* plane) using a commercial FE-package (COMSOL Multiphysics) over a frequency range of 0.5 to 3.0 MHz, using a 0.02 MHz frequency step.

The simulation returns the pressure fluctuation *p*, i.e. the augmented pressure when an acoustic standing wave is set up in the fluid. As demonstrated previously in [6] for 2D models and in [7] for three dimensional ones, the response to excitation of such an acoustic system can be accurately predicted only by taking into account the whole geometry and not by considering the fluid volume only (i.e. assuming the fluid to be resonating between rigid walls). For this reason the fluid-structure interaction has to be taken into account: the solid movement has been coupled to the fluid by equating their accelerations at the wall i.e. $a_n = -\omega^2 \boldsymbol{u}.\boldsymbol{n}_s$, where a_n is the fluid acceleration ω is the frequency of the acoustic wave in the solid, $\boldsymbol{u}$ the solid displacement vector, and $\boldsymbol{n}_s$ the outer normal unit vector of the solid wall. On the other hand, the surface force exerted by the fluid on the solid (pressure *p*) has been included in the model by balancing the pressure to the normal stress, $\sigma_{ns} = -p.\boldsymbol{n}_s$. Damping has been included by using complex stiffness parameters for the glass and complex speed of sound in the water [8].

Fig. 2 shows the predicted absolute pressure amplitude along the lower boundary of the chamber for each of the frequencies examined. The locations of maximum pressure are plotted in red, minimum in blue, so that the pressure nodes appear in green. As a line of particles along the center of the channel is desired in preparation for further mechanical manipulation, the frequencies of interest, marked with black arrows, are 780 and 2140 kHz, at which 1 and 3 lines are formed respectively. In fact, in such a one dimensional pressure field and for the material parameters of the fluid and particles used here, particles are expected to collect at the locations where the pressure fluctuation vanishes ($p = 0$) and the velocity is maximal, as these correspond to the minima of the Gor'kov potential [9], an

expression describing the fluid-particle interaction in form of a force potential for an arbitrary acoustic field and hence defining the trapping locations:

$$\langle U \rangle = 2\pi r_s^{3} \rho \left(\frac{1}{3} \frac{\langle p^2 \rangle}{\rho^2 c^2} f_1 - \frac{1}{2} \langle v^2 \rangle f_2 \right) \tag{1}$$

The terms $\langle p^2 \rangle$ and $\langle v^2 \rangle$ are the mean square of the pressure fluctuation and of the velocity at the particle's location, respectively, whilst the constant terms $f_1 = 1 - \rho c^2 / (\rho_s c_s^2)$ and $f_2 = 2(\rho_s - \rho)/(2\rho_s + \rho)$ take into account the speed of sound in the fluid (c) and in the solid (c_S), as well as their densities (ρ, ρ_S). In a two dimensional approach it suffices to consider the pressure nodes to know where particles will be trapped, as only the component of the velocity vector across the channel is considered, whilst the one along it is neglected, and as this is 180° phase shifted (the velocity can be derived from the pressure through the velocity potential $v = [-\partial\phi/\partial x, -\partial\phi/\partial y]$ using the linear relation $\partial\phi/\partial t = p/\rho$). It has to be said that the model neglects acoustic streaming, secondary radiation forces and drag during migration to the trapping locations, as these play a minor role in the present application.

Fig. 3(a) and (b) show the pressure, the maximum being 0.19 MPa for excitation at 780 kHz and 1.07 MPa at 2140 kHz. As the pressure does not vary considerably in the vertical direction, particles are expected to be found at the bottom of the channel, in parallel lines, as gravity is the only force to which they are subjected in the y-direction. This can be seen in the from the potential U as well.
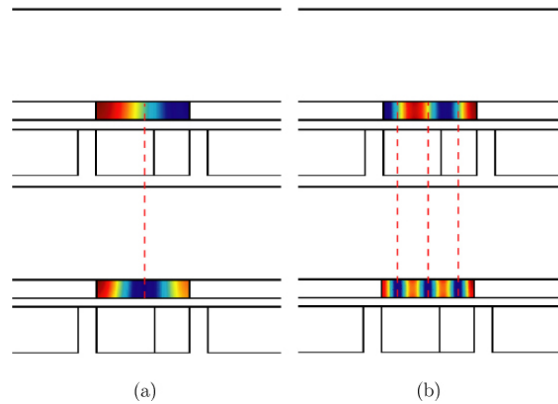

(a)   (b)

Fig.3 Pressure p (top) and force potential U (bottom) in the x-y plane at 780 kHz (a) and 2140 kHz (b). Red indicates the maximum value, blue the minimum

2.3. Experimental results

For the combined manipulation purpose both frequencies can be used in sequence: firstly excitation at 780 kHz to gather all the particles in the center of the channel so that all are accessible to the microgripper, followed by an accurate positioning along the axis by excitation at 2080 kHz.

This is shown in Fig. 4. Three particles are successively removed from the channel and deposited on a glass surface in front of it. Firstly, the system in (a) has been excited at 780 kHz (b-c, taken at 0.5 and 3 s after the beginning of the excitation, respectively), gathering the - at the start randomly distributed - particles in the central region. Then in (d), the frequency was switched directly to 2080 kHz, in order to create a tighter line of single particles. As more particles are present in the potential well than physical space, some are seen to jump on top of each other (marked with arrows), filling the next level of minimum potential. In preparation for the microgripper to

enter the channel, the acoustic field is turned off, as this might set the microgripper into vibration as well, causing undesired effects, such as attraction of particles towards the microgripper fingers (for a detailed description see [6]). The end of excitation can be seen in (e) where the two marked particles in (d) on top of other ones have fallen on the bottom, sliding besides the lower ones. Next, the microgripper is entered into the channel 20 μm above the lower surface at a velocity of 0.2 mm/s, is moved to the position of the first particle, and then the fingers are actuated by applying 90 V (f). The grasped particle is then removed from the fluid and is released on a glass plate, placed in front of the channel in a lower location, this being visible by the refocusing in (g). The fluid surrounding the particle when it is removed revealed to be sufficient to make it adhere to the substrate releasing it from the fingers.
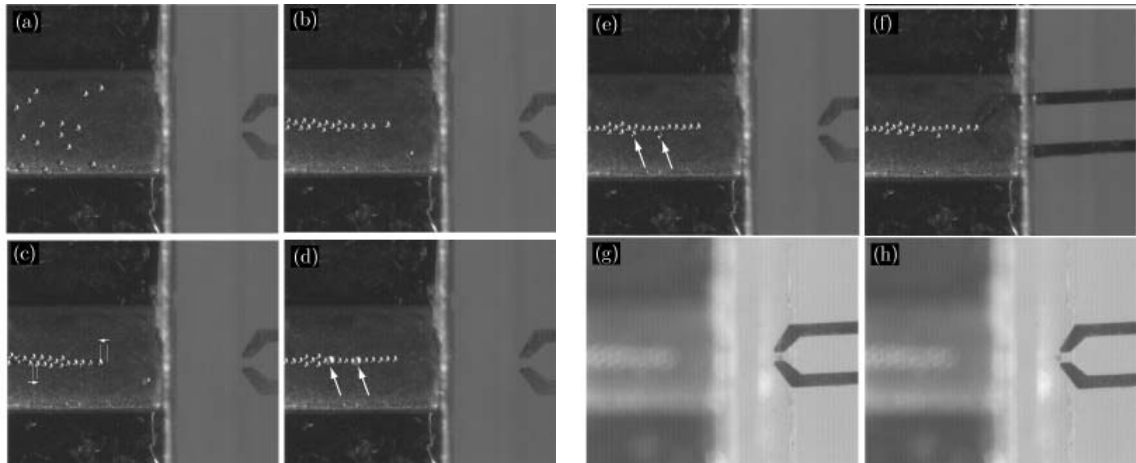

Fig.4 Combined manipulation of a 74 μm copolymer particle. The system is firstly (b) excited at 780 kHz for a crude gathering of all the particles in the central region of the channel and then more accurately positioned by switching the excitation frequency to 2080 kHz (d). Next, in preparation for the microgripper to enter the channel, the acoustic field is turned off, as can be seen by two particles marked with arrows, previously on the top of other two, fallen on the bottom surface (e). Then the microgripper is inserted in the channel and the first particle in the row is grasped (f). After removal from the fluid (g), the microgripper is lowered on a glass surface positioned in front of the channel entrance and the particles released (h). The arrows in (c) mark the displacement of two particles during actuation at 780 kHz in function of the time, (c) and (d) being spaced by 2.5 s.

In order to demonstrate that this process is repeatable, an essential point in demonstrating the automation possibilities of the combination of acoustic positioning and external gripping, the process has been repeated for two further particles. Before the microgripper reentered the channel the acoustic field has been activated again to tighten the line. This way, any lateral misalignment due to motion of the microgripper or to an excessive amount of particles as seen in (e) could be eliminated. It has been observed that there was no need to displace the microgripper across the channel to pick the next particle, this showing the scatter of lateral acoustic positioning. From a detailed investigation it turned out that this amounts to about 14.0 μm. This was obtained by taking the average value for the position measured when the microgripper is in position to grasp the particle, but the fingers still were not actuated. This scatter guarantees that the particle still lies within the fingers of the unactuated microgripper.

The positioning uncertainty in *z*-direction resulted to be higher, 37 μm. This is limited by two factors. First, a gradient in the acoustic field, created by the pressure release boundary at the liquid-air interface, causes a movement of particles along the channel axis. This is shown in (c) by the arrows marking the displacement of two particles with respect to their position in (b) and cannot be predicted by the two dimensional model. Secondly, as seen previously, when more particles are present than the locations of minimum e.g. as in (d), by reactivating the field they might rearrange and squeeze between two particles on the lower level, moving the whole line to the right or to the left.

Finally, a dead volume was observed in proximity of the liquid-air interface where particles cannot be positioned using acoustic forces: as the microgripper has to travel hence a longer distance after each removal process before

coming in contact with the next particles, it is important to reduce this volume and allowing particles to be brought in proximity of the microgripper. This has been done by moving the particles along the channel by means of a laminar flow, as reported in [7].

3. Crystallography sample preparation using nylon loops

3.1. Experimental setup and method

The device consists of a 1 mm wide and 11 mm long channel dry etched to a depth of 200 μm into a silicon wafer sealed on the top with a glass plate (1 mm thick) and provided with a piezoelectric transducer (3×5×0.5 mm) on the bottom (Fig. 5). An orifice (300 μm wide, 700 μm long) has been created in the channel bottom surface to provide access for the loop to the crystals from below (Fig. 5 c, d). A second opening, with a diameter corresponding to the width of the channel, has been etched at one extremity so that a socket to plug in a Teflon tube is created. Two holes, manually drilled in the glass plate, serve as buffer solution reservoir and inlet for the sample. For operation buffer solution is flushed through the device by loading it in the reservoir and using a syringe pump (kDScientific, KS270) to withdraw fluid from the other extremity. A small droplet of sample is then introduced by means of a pipette through the second hole in the glass plate. The use of two inlets ensures that all the injected crystals are exposed to the velocity field; hence losses of sample are minimized. Once the crystals have been aligned along the centerline by exciting the piezoelectric element, they are moved along the channel towards the orifice until a crystal falls into it. Then the loop is introduced from below, the crystal is trapped and removed. Surface tension forces on hand prevent leakage from the orifice and on the other hand keep the crystal in the droplet confined within the perimeter of the loop allowing transfer to a N_2 container for freezing. The process is observed from above through the microscope. As for the previous application, a *xyz* positioning system is used to move the loop. The device is clamped using a plastic holder.

3.2. FE-Modeling (3D)

As the acoustic field between the specimen inlet (6) and the orifice (4) is of interest, a three dimensional model is necessary, which takes into account the boundary conditions for the fluid. Zero pressure fluctuation has been set (pressure release boundary) there, which is a realistic assumption considering the large disparity in acoustic impedances. At the other boundaries (channel cross section) zero pressure gradient has been assumed, given the fact that only the central region far from the channel ends is of interest here. The force potential *U* is shown in Fig. 6 in form of isolines, with blue marking the minima. It can be seen that crystals are indeed aligned along the centerline, but cannot be positioned in proximity of the orifice using acoustic forces. This limitation is bypassed by the use of the laminar flow regime which occurs in microchannels, which ensures that the lateral position achieved with acoustics is kept down to the orifice. This finding about the trapping locations is due to the fact that now the dependence of *p* from the *y*-position is taken into account. Furthermore acoustic forces acting along the channel (in the literature also known as lateral forces) pull the crystals along the channel towards its center. These forces arise direct from the $\langle v^2 \rangle$ term in the force potential, as now also the component along the channel axis of the velocity vector is considered. Although the results reported here have been calculated for spherical copolymer particles with a diameter of 100 μm (c_S = 3000 m/s, r_S = 1050 kg/m^3) the same type of particles used in [1]) the predicted trapping locations are representative. It has to be mentioned that even though small crystals or fragments of larger crystals have been seen floating as consequence of acoustic streaming, rather than moved by acoustic radiation forces, streaming has been neglected in the model as only the larger crystals are of interest for the present application.
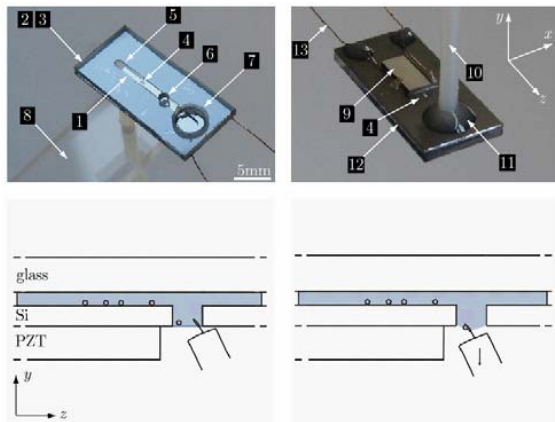
Fig.5 Top (a) and (b) bottom view of the acoustic device used for crystal manipulation. A channel (1) etched in silicon (2) is filled with buffer solution loaded in a reservoir (7) defined in the glass plate used for sealing (3). Crystals are inserted by means of a pipette through the inlet (6) and transported in the acoustically active region (the region over the piezoelectric transducer, 9) by creating a flow along the channel using a syringe pump and a Teflon pipe (10) plugged into a socket at the extremity (5) of the channel on the backside and fixed using glue (11). Once a crystal has fallen in an orifice defined on the bottom surface of the channel (as shown in the cross section c and d), a nylon loop is inserted from below, moved above the crystal, lowered in the negative *y*-direction against the liquid meniscus until the surface tension is overcome and the crystal remains confined in the droplet trapped in the nylon loop. The piezoelectric transducer is run by connecting its electrodes to a function generator and an amplifier (12). The device is clamped under a microscope using a plastic holder (8).
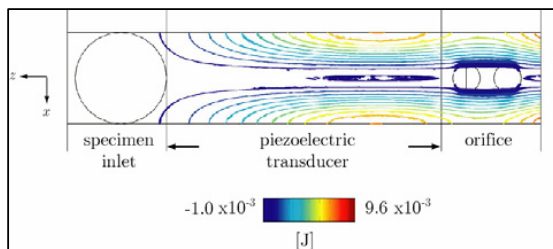

Fig.6 Force potential field U (depicted as isolines) at 7543 kHz for the central region of the channel, between the specimen inlet and the orifice. Particles are trapped along the centerline but not in proximity of the orifice.
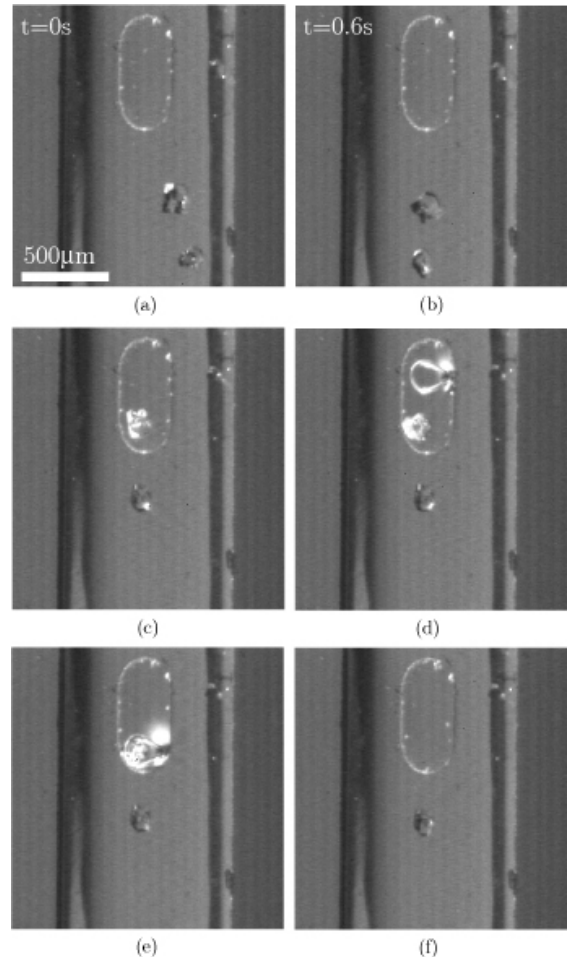

Fig.7 Crystal manipulation process. After having being loaded into the channel through the specimen inlet, crystals are brought in the region above the transducer (a), by applying a flow of 0.05 ml/s (from bottom to the top in the figure). The transducer is responsible for aligning the crystals along the centerline when excited at 751 kHz (b). Next, the flow is applied again (c) until a crystal falls into the orifice (d). Then the loop is inserted from below, moved above the crystal and pulled down until the crystal is removed from the liquid (e-f). The crystal remains confined in the droplet of buffer solution trapped in the loop.

3.3. Experimental results

The whole manipulation process is shown in Fig. 7. After crystals have been inserted through the specimen inlet and transported into the acoustically active zone by applying a flow of 0.05 ml/s (a), the acoustic field is excited at 751 kHz (b). All the crystals are thereby positioned along the centerline. A fluid flow is then applied until a crystal

has fallen into the orifice (c). The loop is at this point inserted from below (as indicated in Fig. 5) and the crystal removed (e-f).

Due to the irregular shape of the crystals, some of them might rotate during application of the ultrasound but still keep the position in the middle of the channel in *x*-direction. Furthermore, as consequence of the large differences in the size of the crystals, the flow has the beneficial effect of spreading them out along the channel. However, it might be also detrimental as some crystals traveling faster than others might overtake them creating a clump or losing lateral position. In such cases a short application of ultrasound would be necessary to position them again on the centerline, as used above. For this experiment the use of two frequencies, as done before, was not necessary.

Finally, a comment about acoustic streaming has to be made. Even though this might be detrimental in most positioning applications, it can be indirectly exploited here to improve the performance of the device, as only large undamaged crystals are manipulated.

4. Conclusions

The manipulation of large single particles using acoustic radiation forces in combination with laminar flow, surface tension and external tools such as microgrippers and loops has been shown here. In specially designed systems particles are positioned in a line along the centerline so that they can be individually accessed by an external tool in the channel axis direction. The tool is inserted through the liquid meniscus created at the liquid-air interface, which characterizes these systems.

Aknowledgements

References

[1] A. Neild, S. Oberti, and J. Dual, "Design, modeling and characterization of microfluidic devices for ultrasonic manipulation," Sens. Actuators B, 121, pp.452-461, 2007
[2] J. Hultström, O. Manneberg, K. Dopf, H.M. Hertz, H. Brismar, M. Wiklund, "Proliferation and viability of adherent cells manipulated by standing-wave ultrasound in a microfluidic chip," Ultrasound in Medicine & Biology, 33, pp. 145-151, 2007
[3] N. R. Harris, M. Hill, M.S. Beeby, Y. Shen, N. M. White, J. J. Hawkes, and W. T. Coakley, "A silicon microfluidic ultrasonic separator, " Sens. Actuators B, 95, pp.425-434, 2003
[4] F. Petersson, A. Nilsson, C. Holm, H. Jönsson, and T. Laurell, "Continuous separation of lipid particles from erythrocytes by means of laminar flow and acoustic standing wave forces, " Lab Chip, 5, pp. 20-22, 2005
[5] F. Beyeler, A. Neild, S. Oberti, D. J. Bell, Y. Sun, J. Dual, and B. J. Nelson, "Monolithically Fabricated Microgripper With Integrated Force Sensor for Manipulating Microobjects and Biological Cells Aligned in an Ultrasonic Field," J. Microelectromech. Systems, 16, pp. 7-15, 2007
[6] A. Neild, S. Oberti, F. Beyeler, J. Dual, and B. J. Nelson, "A micro-particle positioning technique combining an ultrasonic manipulator and a microgripper," J. Micromech. Microeng., 16, pp.1562-1570, 2006
[7] S. Oberti, A. Neild, D. Möller, J. Dual, „Towards the automation of micron-sized particle handling by use of acoustic manipulation assisted by microfluidics," Ultrasonics, 48, pp. 529-536, 2008
[8] M. Gröschl, "Ultrasonic separation of suspended particles. Part I. Fundamentals," Acustica, 84, pp.432-447, 1998
[9] L. P. Gor'kov, "Forces acting on a small particle in an acoustic field within an ideal fluid," Doklady Akademii Nauk Sssr, 140, pp.88-92, 1961